University of Minnesota
ST. ANTHONY FALLS HYDRAULIC LABORATORY

Project Report No. 157

HYDRAULIC TRANSIENT ANALYSIS FOR THE CULVER-GOODMAN TUNNEL ROCHESTER, NEW YORK

by
Charles C.S. Song,
Timothy M. Ring,
Alwin C.H. Young,
and
Kim S.G. Leung

Prepared for
LOZIER ENGINEERS, INC.
Rochester, New York

December 1975
Minneapolis, Minnesota

ABSTRACT

This report describes a mixed-flow hydraulic transient model for the Culver-Goodman Tunnel of Rochester, New York. The model is based on the one-dimensional unsteady partial differential equations for open channels and closed conduits. These differential equations are solved numerically using the method of characteristics. Thus, the model is capable of dealing with the rapidly changing water hammer pressures and surges in a complex system. Hydrographs at 18 dropshafts due to a 5 year storm are used as the inputs. Outflow hydrographs, storage, depth or piezometric head, and velocity at 104 stations at small time intervals are obtained as output.

CONTENTS

Hydraulic Transient Analysis for the Culver-Goodman Tunnel Rochester, New York

I. INTRODUCTION

The Culver-Goodman Tunnel is designed to carry the combined sanitary flow and the surface runoff from an estimated 5-year storm from its service area. The flow is to be discharged into the Cross-Irondequoit Tunnel. Tentative lay-out and sizing of the tunnel were based on an extensive hydrologic and hydraulic analysis performed by Lozier Engineering, Inc., in cooperation with Dorsch Consult, Ltd. According to their calculations, the maximum discharge at station 5000 would be 2,462.2 cfs with no control at the downstream end. This maximum discharge might increase considerably if the system is to receive the flow from the Norton Street Tunnel (station 1308) and/or from other drainage areas at some future time.

A question has been raised as to whether the Cross-Irondequoit Tunnel can carry the maximum flow from the Culver-Goodman Tunnel as indicated by the preliminary design. That is, there is a possibility that the outflow from the Culver-Goodman Tunnel has to be limited. This would require a flow control structure at the downstream end of the Culver-Goodman Tunnel. In regulating the outflow, the control structure must be designed in such a way that (1) no excessive hydraulic transient pressure is generated anywhere in the system, (2) none of the dropshafts overflow, and (3) the storage capacity of the tunnel is utilized effectively. It is also necessary to find whether off-line storage capacity is needed in order to reduce total overflow if the outflow rate is severely limited. The purpose of the analysis reported herein is to develop a computer program that is capable of simulating the transient flow characteristics of the system under various flow constraints.

A very complex and accurate mathematical model is needed to accomplish this purpose. Not only is the geometry of the system fairly complex; it is also necessary to deal with open channel and closed conduit transients simultaneously. The computations must be carried out in sufficient detail so that maximum and minimum transient pressures due to water hanner and surges throughout the system are determined.

A transient mixed-flow mathematical model based on the method of characteristics was developed. This report describes the model and some preliminary output based on this model.

II. DESCRIPTION OF THE MATHEMATICAL MODEL

A. Basic Equations

The basic differential equations governing a one-dimensional open channel flow are the equation of continuity [1]*,

$$\frac{\partial y}{\partial t} + V \frac{\partial y}{\partial x} + \frac{A}{T} \frac{\partial V}{\partial x} = 0 \qquad (1)$$

and the equation of motion,

$$g \frac{\partial y}{\partial x} + \frac{\partial V}{\partial t} + V \frac{\partial V}{\partial x} + g(S_f - S_o) = 0 \qquad (2)$$

The corresponding equations for a closed conduit flow are the equation of continuity [1],

$$\frac{\partial H}{\partial t} + V \frac{\partial H}{\partial x} + \frac{a^2}{g} \frac{\partial V}{\partial x} = 0 \qquad (3)$$

and the equation of motion,

$$g \frac{\partial H}{\partial x} + V \frac{\partial V}{\partial x} + \frac{\partial V}{\partial t} + g(S_f - S_o) = 0 \qquad (4)$$

Lateral inflows through dropshafts do not appear in these equations, because they are regarded as point inflows and will be treated when considering dropshaft boundary conditions.

The meanings of the symbols used in the above equations are as follows:

A = cross-sectional area of the flow
a = speed of pressure waves in closed conduit flow
g = gravitational acceleration
H = piezometric head measured from the bottom of the tunnel
S_o = slope of the tunnel
S_f = energy slope which may be computed by means of Manning's equation
t = time
T = width of water surface
V = flow speed
x = distance along the tunnel
y = depth of flow

---

*Number in brackets refer to the List of References on page 16.

A number of approaches can be used to solve the differential equations listed above. Among these alternative approaches, the implicit method and the characteristic method stand out in recent literature as the favorite methods. For open channel flood routing problems, there is a tendency to favor the implicit method as being computationally more efficient [2, 3, 4]. This is due to the fact that the implicit method is numerically more stable and permits the use of larger time steps. In other words, for a relatively slowly varying transient open channel flow, the implicit method is preferable. However, for the rapidly varying transient flow considered herein, the simpler characteristic method is preferable, and the implicit method loses its advantage because very small time steps are required to determine the maximum and minimum transient pressure. Thus, the characteristic method is adopted for reasons of simplicity.

The characteristic equations representing Eqs. 1-4 for open channel flows are,

$$\frac{dx}{dt} = V \pm C \tag{5}$$

$$\frac{dy}{dt} \pm \frac{C}{g}\frac{dV}{dt} \pm C(S_f - S_o) = 0 \tag{6}$$

and for closed conduit flows,

$$\frac{dx}{dt} = V \pm a \tag{7}$$

$$\frac{dH}{dt} \pm \frac{a}{g}\frac{dV}{dt} \pm a(S_f - S_o) = 0 \tag{8}$$

where $C = \sqrt{\frac{gA}{T}}$ (9)

is the speed of the gravity wave and a is the speed of the pressure wave in a closed conduit.

B. System Configuration

The general layout of the Culver-Goodman Tunnel is shown in Fig. 1. For the purpose of numerical analysis, the tunnel is divided into 102 sections of roughly 300 ft each in length. These sections are adjusted, whenever necessary, so that all dropshafts and junctions are located at the end points of these sections. Two fictitious sections have been added at the upstream end of the west branch (Goodman Street) so as to take into account the effect of possible future extensions of the tunnel.

The tunnel is assumed to have a constant (16 ft) diameter circular section, a constant slope (0.001), and a constant Manning's friction coefficient n (0.013). For the preliminary computations, all dropshafts are assumed to consist of vertical 8 ft diameter pipes. (The diameter of some dropshafts may subsequently have to be increased so that they may serve as surge tanks.) Inflow hydrographs at all 18 dropshafts including the one that receives the flow from Norton Street Tunnel are given.

There will be a discharge control and a diversion structure located at the downstream end. Initially, the discharge control was assumed to be of a sluice gate type, although other types of flow control devices may be considered later. For diversion, a weir type structure is assumed.

C. Finite Difference Equations

A fixed grid system characteristic method [1] is adopted. For given $\Delta x = 300$ ft, the time step Δt has to be chosen so that the following stability criteria are met for open channel flows,

$$\Delta t \leq \Delta x / |V \pm C| \tag{10}$$

and for closed conduit flows,

$$\Delta t' \leq \Delta x / |V \pm a| \tag{11}$$

When mesh sizes are chosen according to the above stability criteria, the characteristic lines issuing from a nodal point P will intersect the line representing the previous time as shown in Fig. 2. These intersects are denoted R and S in Fig. 2. Accordingly, the characteristic differential equations, Eqs. (6) and (8), can be written as:

for open channel flows,

$$C^+ : y_P - y_R + \frac{C_R}{g}(V_P - V_R) + C_R(S_f - S_o)_R \Delta t = 0 \tag{12}$$

$$C^- : y_P - y_S - \frac{C_S}{g}(V_P - V_S) - C_S(S_f - S_o)_S \Delta t = 0 \tag{13}$$

and for closed conduit flows,

$$C^+: H_P - H_R + \frac{a}{g}(V_P - V_R) + a(S_f - S_o)_R \Delta t' = 0 \qquad (14)$$

$$C^-: H_P - H_S - \frac{a}{g}(V_P - V_S) - a(S_f - S_o)_S \Delta t' = 0 \qquad (15)$$

Subscript P, R, and S represent the points shown in Fig. 2.

When the flow at the nodal points A, B, and C are known, then the corresponding values at the intersects R and S can be obtained by linear interpolations. In principle, a set of unknown (y_P, V_P) or (H_P, V_P) can be readily obtained by solving Eqs. (12) and (13) or Eqs. (14) and (15), respectively.

It is expected that, during certain time periods, a portion of the tunnel may be filled while the remaining portion will operate as an open channel. Since a is much greater than C in general, $\Delta t'$ has to be much less than Δt. In this case, the resulting grid system will be like the one indicated in Fig. 3. This figure indicates a case when the upstream section AC is an open channel and the downstream section CB is a closed conduit. For a mixed flow condition like this, a predetermined time step Δt for the open channel flow portion must be subdivided into n units of $\Delta t'$ such that

$$\Delta t' = \frac{\Delta t}{n} \leq \Delta x / |V \pm a| \qquad (16)$$

Values at the intermediate steps represented by P', C', B', etc., are to be computed before the values at the point P can be computed. That is, for every step of computation for open channel flows, a set of n intermediate step computations must be performed for the closed conduit portion of the system. For the specific case indicated in Fig. 3, the appropriate set of equations to be used for P' are Eqs. (12) and (15). The complete set of solutions are obtained by marching forward in time starting from a known initial condition in the manner prescribed above.

D. Determination of Phases

For a given set of typical inflow hydrographs, the flow in the tunnel will first increase and then decrease as time passes. Thus, at a typical station, the flow will change from an open channel phase to a closed conduit phase and

back to an open channel phase. Very little information is available at the present time as to the precise manner in which the phase change will occur. Past analytical and experimental workers have tried to avoid this difficult question by treating closed conduit flow and open channel flow separately. For example, Anderson and Dahlin [5] conducted a transient model test of a simple dropshaft system for the purpose of verifying a mathematical model being developed by Harza Engineering Company. The model consisted a five dropshafts attached to a straight tunnel. The upstream end of the tunnel was a dead end and the downstream end was attached to a tailwater level control box. Thus, the tunnel was maintained at full condition during the transient experiment. A nearly rectangular-shaped inflow hydrograph was introduced into one of the dropshafts and the resulting surges at the remaining four dropshafts were measured.

One problem related to the phase change concerns the speed of the gravity wave as defined by Eq. (9). As the flow depth approaches the tunnel diameter in the open channel phase, C as given by Eq. (9) approaches infinity. This is physically impossible. In reality, as C approaches a the pressure wave should take over as the primary medium for the propagation of disturbances. Furthermore, open channel flow with an extremely small air space above the water surface is likely to be very unstable because of the difficulty in maintaining the required air flow rate. For this reason, a phase change during a rising period is assumed to occur at a depth slightly less than D so that the flow is regarded as open channel when

$$y \leq D - \epsilon \tag{17}$$

but closed conduit when

$$y > D - \epsilon \tag{18}$$

The value for ϵ at which the actual phase change occurs may depend on such factors as the amount of air entrainment and the magnitude of flow disturbances. The value of $\epsilon = 0.01$ ft and 0.05 ft were tried and both appeared to yield reasonable results, although the larger value resulted in a significant saving on computer time.

The phase change criteria stated above worked well for the transition from the open channel condition to the closed conduit condition. The problem is more complicated during the falling period when the flow phase changes from closed

conduit to open channel. Water hammer waves characterized by fast rising and falling head exist in the closed conduit portion of the transient flow. These water hammer waves are often of sufficient magnitude to temporarily lower the head below the diameter of the tunnel. Depending on the level of the minimum head and the amount of entrained air, water hammer may cause column separation or cavitation. Clearly, there is a need to distinguish the true open channel flow from a temporary drop in head due to a water hammer wave. Since no information is available in the literature concerning the detailed mechanism of phase change from closed conduit to open channel flow, the mathematical model will be written under an assumption that "the transition from closed conduit flow to open channel flow requires so much air that it can take place only when the station is ventilated." Thus, the stations where a transition from closed condition to open condition is permitted are the upstream and downstream ends, dropshafts, and interfaces. Any interior station within the closed conduit flow portion is not allowed to open up even if the computed head drops below $D - \epsilon$.

In summary, the model assumes that the flow may change from open condition to closed condition whenever the computed depth exceeds $D - \epsilon$ but not in reverse. Flow can first open up only at the end stations and the dropshafts so that, as the flow continues to decrease, the open channel portion will gradually expand by allowing the interface to move in an orderly manner.

E. Boundary Conditions

1. Upstream End

Two types of upstream boundaries, an open end that extends indefinitely far upstream, and a closed end with a dropshaft attachment are considered. In either case, the inflow Q is known.

For an open end,

$$Q = AV \tag{19}$$

is given. In addition to Eq. (19) there is available a negative characteristic equation, Eq. (13) or Eq. (15), depending on whether the flow is open or closed.

For a closed end with dropshaft the treatment is similar to that of the dropshaft boundary condition explained later.

2. Downstream End

During the initial stage of the analysis only a sluice gate type control structure is assumed. The downstream end of the circular tunnel is assumed to be connected to a rectangular outlet through a smooth transition. The sluice gate opening is characterized by its width B and height b. Various cases, depending on whether the flow is open or closed and whether the gate is controlling or not, have to be considered.

A positive characteristic equation is first selected according to whether the flow is open or closed. Next a flow rate equation is selected depending on whether

$$\frac{V^2}{2g} + y \leq \frac{3}{2} b \tag{20}$$

or $$\frac{V^2}{2g} + y > \frac{3}{2} b \tag{21}$$

When Eq. (20) is applicable, then the gate is not controlling and the flow at the exit is critical. In this case the governing equation is

$$Q = C_d B \left(\frac{V^2}{2g} + y\right)^{3/2} \tag{22}$$

where $C_d = 3.089$. When Eq. (21) is satisfied, then the gate is controlling and the flow rate equation is [6]

$$Q = C_d' \, b B \left(\frac{V^2}{2g} + y\right)^{1/2} \tag{23}$$

where $C_d' = 4.634$.

3. Dropshaft

When the water depth at a dropshaft station is less than $D - \epsilon$, then the dropshaft is not actively participating in the transient flow. Conversely, if the flow depth is greater than $D - \epsilon$, then the dropshaft will act as a surge tank. Figure 4(a) represents the former case and Fig. 4(b) is a typical sketch of the latter case. Lateral inflow Q is treated as a point input.

For open channel flow as shown in Fig. 4(a), the station is represented by two substations separated by a negligibly small distance. The depths at these substations are assumed equal but the velocities are necessarily different to accommodate the lateral inflow. The three unknowns, y_P, V_{1P}, and V_{2P} are obtained by solving Eqs. (12), (13), and the equation of continuity,

$$Q_P + V_{1P}A(y_P) = V_{2P}A(y_P) \tag{24}$$

There are four alternate flow conditions possible when the dropshaft is acting as a surge tank. Figure 4(b) indicates one of these when neighboring sections are both closed. (The others involve different combinations of open and closed sections.) The four unknowns, H_P, V_{1P}, V_{2P}, and V_{3P} are obtained by solving Eqs. (14), (15), the equation of continuity,

$$V_{3P} + \frac{D^2}{d^2}(V_{1P} - V_{2P}) = 0 \tag{25}$$

and the storage equation,

$$\frac{2(Q_C + Q_P)}{\pi d^2} - \frac{V_{3C} + V_{3P}}{2} = (H_P - H_C)/\Delta t' \tag{26}$$

Similar equations are used for the other three flow conditions except that an appropriate set of characteristic equations must be selected for each condition.

4. Junction

For the purpose of simplification the dropshaft located at a junction is shifted downstream by one station. The junction station is represented by three substations associated with each of the three branches of the tunnel system. There are four unknowns, y_P, V_{1P}, V_{2P}, and V_{3P} to be solved using three characteristic equations and a continuity relationship. The main problem here is to select an appropriate set of characteristic equations compatible with the flow conditions in the adjacent sections. Eight possible combinations must be considered here.

III. NUMERICAL RESULTS

A. Input Data

1. Inflow Hydrograph

All inflow hydrographs including that of the Norton Dropshaft given at 5 minute intervals were used. Intermediate values were calculated by linear interpolation as needed. A constant amount of base flow, 14.15 cfs in each branch and 28.30 cfs downstream of the junction, was assumed before the start of the storm runoff. This was to avoid the computational difficulty that might arise due to zero flow.

2. Downstream Control

Two sluice gates, one 4 ft wide and one 8 ft wide, are assumed to exist at the downstream end. Initially the 4 ft gate is assumed to be fully open but the 8 ft gate is closed. When the discharge exceeds 150 cfs then the 4 ft gate would be closed and the 8 ft gate would open fully. The maximum opening of both gates is assumed to be 16 ft.

3. Pressure Wave Speed

It is well known that the speed of a pressure wave is very sensitive to the free air content of the water [1]. It takes the maximum value of 4,500 fps for pure water and decreases rapidly as the free air content increases. For example, the wave speed is 2,000 fps at 0.1 percent concentration by volume and 1,000 fps at 0.45 percent concentration. It is expected that the air concentration in the system will be rather high due to the high rate of air entrainment in dropshafts. However, there are no data that can be used to even estimate the amount of air concentration that may exist in the system.

Lacking the data on air concentration, the value of $a = 1{,}000$ fps was chosen for a complete computational run. This is followed by a partial run using $a = 2{,}000$ fps for the purpose of sensitivity analysis.

B. Outflow Hydrograph and Storage

The variation of discharge at the downstream end and the total volume of water stored in the system are plotted as functions of time in Fig. 5. This

figure indicates that the discharge initially increases very slowly, reaching 150 cfs at t = 87.38 minutes. At this instant, the 4 ft sluice gate is suddenly closed and the 8 ft gate is open. The result is a jump in discharge as can be observed in the graph. Discharge increases very rapidly thereafter and reaches the maximum value of 2,415 cfs at t = 112.50 minutes. Before the discharge reaches its maximum value, however, the tunnel at a station midway between the Norton Dropshaft and the sluice gate first becomes filled at t = 110.07 minutes. The flow thus becomes of a mixed type and water hammer waves and surges begin to appear. This mixed flow regime lasts until t = 166 minutes and, thereafter, the flow returns to an open channel flow for the falling part of the hydrograph.

Clearly the rising and the falling parts of the hydrograph are characterized by an open channel flow, whereas for a relatively constant discharge a mixed-flow regime prevails. There is a sharp peak discharge at t = 112.50 minutes, which roughly coincides with the time of maximum inflow at the Norton Dropshaft. This is accompanied by many surges, as indicated more clearly in Fig. 6. In this figure, the discharge hydrograph for an 8-minute period is plotted using a larger time scale. It shows a pulsating discharge of amplitude equal to 300 cfs and period equal to 1/2 minute. Several minutes after the peak, the discharge settles down to a nearly constant value of approximately 1,700 cfs for the rest of the mixed flow phase.

The curve in Fig. 5 showing the variation of total water stored in the system is very smooth. It rises rapidly after t = 90 minutes to the maximum value of 5.65 million cubic ft at t = 132 minutes. From there on the storage drops gradually, even though the discharge remains fairly constant during the mixed-flow phase. The maximum storage attained is approximately equal to 94 percent of the system's storage capacity. Perhaps, with some adjustments, 100 percent of the storage capacity may be utilized and the maximum outflow can be reduced to the neighborhood of 2,000 cfs without overflowing the system.

C. Depth or Head

During the rising phase of the hydrograph the flow depth increases gradually from its base value of 1 ft upstream of the junction and of 1.307 ft downstream of the junction. This gradual change in the flow depth continues until t = 110.07 minutes, the instant when the tunnel is first filled near the downstream end. The hydraulic gradeline on the Goodman Street Tunnel at this instant

is shown in Fig. 7 as curve 1. This curve clearly indicates that the flow is restricted at two locations, the junction and the end sluice gate. Particularly significant is the existence of a back water curve due to the restriction at the junction, which would be filled first if the inflow from Norton Dropshaft was excluded.

The existence of water hammer waves greatly complicates the hydraulic gradeline during the mixed-flow phase. It changes radically from instant to instant. Curve 2 in Fig. 7 is the hydraulic gradeline at the instant when the maximum head of 103 ft occurred at the junction when $a = 2{,}000$ fps was used. That the dropshafts serve to moderate the transient pressure head can be seen from this curve. Curve 3 is a straight level line shown for reference purposes.

Generally speaking, there are severe water hammer pressure fluctuations at locations where the closed conduit flow condition exists. However, the head fluctuations at dropshafts are significantly reduced due to the surge tank effect. Figure 8 is the time record of the piezometric head at the Norton Dropshaft, where the solid line is for $a = 1{,}000$ fps and the dotted line is for $a = 2{,}000$ fps. Although there are some minor fluctuations, the water surface level is fairly stable at about 16 ft during the whole mixed-flow phase. In comparison, Fig. 9 shows greater head fluctuation at the junction. Since water hammer is a very rapid phenomenon, its effect is not fully and accurately shown in this plot using a small time scale. To show more completely the effect of water hammer, a small portion of the head record at the junction is expanded and plotted in Fig. 10 ($a = 1{,}000$ fps) and Fig. 11 ($a = 2{,}000$ fps). Comparison of these two figures clearly shows that both the frequency and the amplitude of water hammer waves are about doubled when the wave speed is doubled.

It is also interesting to note that there are two types of oscillations, damped simple harmonic oscillations during the initial period and damped composite harmonic oscillations in the later period. This change from a simple harmonic oscillation to a composite harmonic oscillation is due to the fact that the number of sections upstream of the junction having a closed conduit flow condition increased by one at $t = 4$ seconds.

The maximum water hammer pressure in this system occurs a short distance upstream of the Master Street pump station. Figures 12 and 13 are the plots of the water hammer wave at a station 600 ft upstream of the Master Street pump station for $a = 1{,}000$ fps and $a = 2{,}000$ fps, respectively. Again, both the

amplitude and frequency are roughly doubled when the wave speed is doubled. The large negative pressures indicated in these figures are unrealistic but significant. In the real case a large negative pressure would cause column separation (or cavitation) which is not treated in this model. Column separation is very damaging and should be avoided if possible. To show the moderating effect of a dropshaft, the head at the Master Street pump (station 5100) station is plotted as a dotted line in Fig. 13. Contrast between the two plots in this figure is striking. The severe water hammer wave nearby has practically no effect on the head at the dropshaft.

D. Flow Velocity

The flow is subcritical and the velocity profile is continuous except at the dropshafts and the junction. There are step changes in velocity at the dropshafts and the junction as exemplified by Fig. 14, showing the velocity profile in the system at $t = 78.241$ minutes. At this early stage, the difference in discharge between two branches is large enough to cause backflow at the Goodman Street Tunnel near the junction. This backflow starts at $t = 63.822$ minutes and lasts for about 25 minutes. Though it is possible that the flow immediately upstream of a dropshaft may take a negative value, the base flow assumed for this computation run was large enough to prevent this from happening.

IV. CONCLUSIONS AND RECOMMENDATIONS

A transient mathematical model capable of simulating water hammer waves and surges as well as gradually varied mixed-phase flows is now operational. This mathematical model is a powerful tool to aid in the design of the Culver-Goodman sewer system or any other similar storm sewer system.

A complete run of detailed computations was carried out and is reported herein. For this computation, the outlet condition was assumed to be that of an 8 ft wide sluice gate fully open when the discharge exceeds 150 cfs. Following is a list of significant conclusions that can be derived from this study:

1. The outflow hydrograph consists of a rising phase, a constant or holding phase, and a falling phase. The flow is an open channel type during the rising and the falling phase but it is characterized as mixed-flow during the constant phase. The maximum discharge is 2,415 cfs.

2. 94 percent of the total storage capacity is utilized. A better gate design may possibly increase the maximum storage to 100 percent of capacity and reduce the maximum discharge to near 2,000 cfs without overflow occurring in the system. Further reduction of the maximum discharge would require off-line storage or an overflow structure.

3. A dropshaft is a very effective device for reducing water hammer pressure and surges. Additional dropshafts or surge tanks might be required to reduce water hammer waves at critical locations.

4. Water hammer pressure is greatest a short distance upstream of the Master Street pump station. The computation indicates the possibility of column separation occurring there. With the assumed system configuration wherein the dropshaft at the junction was shifted 300 ft downstream, water hammer pressure at the junction is also rather severe. This severe pressure fluctuation may be reduced when the dropshaft is placed at the junction.

5. The magnitude and frequency of the water hammer waves are roughly proportional to the pressure wave speed "a." Since the pressure wave speed is very sensitive to the amount of free air entrained in the water, there is no way to determine "a" accurately at this time.

6. Surges in the dropshafts are relatively unaffected by the values of "a" chosen.

7. There is a possibility that backflow may occur at the junction or at one of the dropshafts, depending on the inflow hydrographs and the base flow assumed. Although the present model indicates backflow may occur at the Goodman Street Tunnel, a different input hydrograph may cause backflow at the Culver Street Tunnel.

The following recommendations are made, based on this study.

1. Additional computational runs using different downstream gate designs should be carried out to seek improved efficiency of the design.

2. A computation should also be carried out using a different inflow quantity coming from the upstream end of the Goodman Street Tunnel. This would give information on the effect of future expansion.

3. If a maximum outflow of less than 2,000 cfs is required, then the effect of an overflow structure and/or off-line storage should be examined.

4. It may be desirable to add one or two surge tanks to the system to reduce the water hammer pressure at critical locations. Some other devices such as a flexible bag may also be considered.

5. Since the mathematical model is based on some likely but unproven assumptions, a transient model test should be carried out to verify the mathematical model. The manner in which the flow phase changes when head changes and the speed of pressure waves in the system are the two most critical uncertainties. Both are closely related to the air entrainment condition at the dropshafts. Another uncertainty of considerable importance is the amount of energy loss at different locations for different flow conditions.

6. From the viewpoint of reducing water hammer pressure, it is advantageous to keep the air concentration at a relatively high level.

7. The present mathematical model could be modified and used for other similar proposed systems.

LIST OF REFERENCES

[1] Streeter, Victor L., and Wylie, E. Benjamin, Hydraulic Transients, McGraw-Hill Book Company, New York, 1967.

[2] Price, Roland K., "Comparison of Four Numerical Methods for Flood Routing," Journal of the Hydraulics Division, American Society of Civil Engineers, Vol. 100, No. HY 7, July 1974.

[3] Amein, M. and Fang, C.S., "Implicit Flood Routing in Natural Channels," Journal of the Hydraulics Division, American Society of Civil Engineers, Vol. 96, No. HY 12, December 1970.

[4] Amein, M. and Chu, H.L., "Implicit Numerical Modeling of Unsteady Flows," Journal of the Hydraulics Division, American Society of Civil Engineers, Vol. 101, No. HY 6, June 1975.

[5] Anderson, Alvin G. and Dahlin, Warren Q., Model Studies - Lawrence Avenue Sewer System, City of Chicago, St. Anthony Falls Hydraulic Laboratory Project Report No. 100, October 1968.

[6] Rouse, Hunter, Elementary Mechanics of Fluids, John Wiley & Sons, Inc., 1947, p. 87.

LIST OF FIGURES

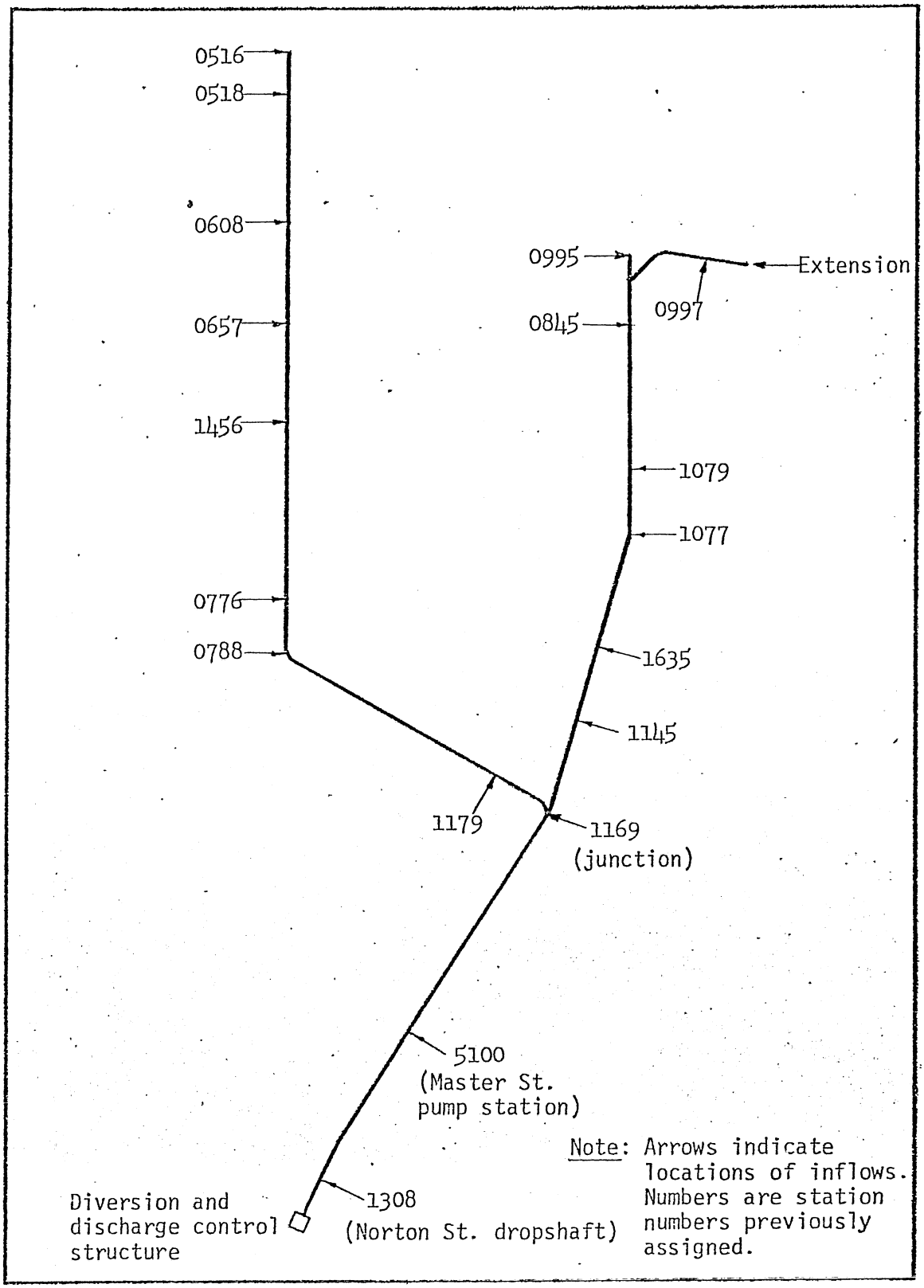

Fig. 1 - General Layout of the Culver-Goodman Tunnel.

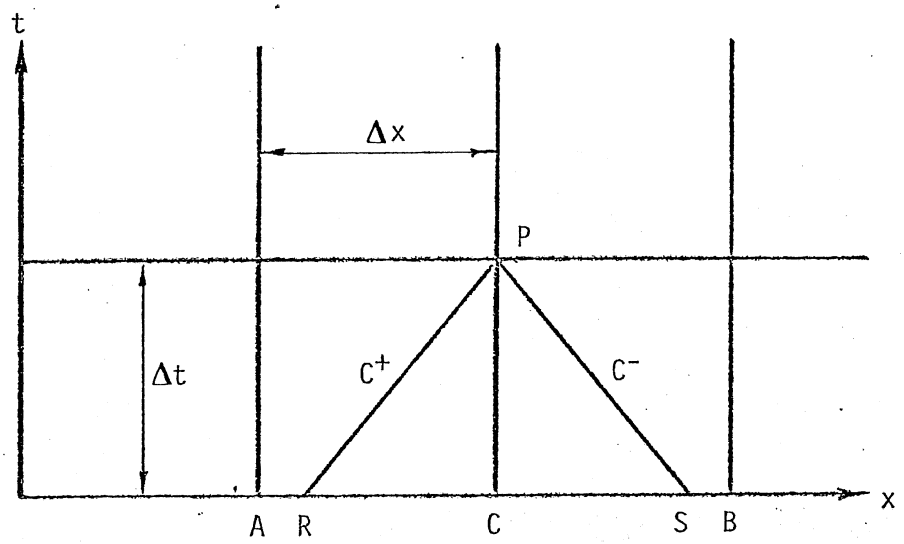

Fig. 2 - Fixed Grid System for Single Phase Flow.

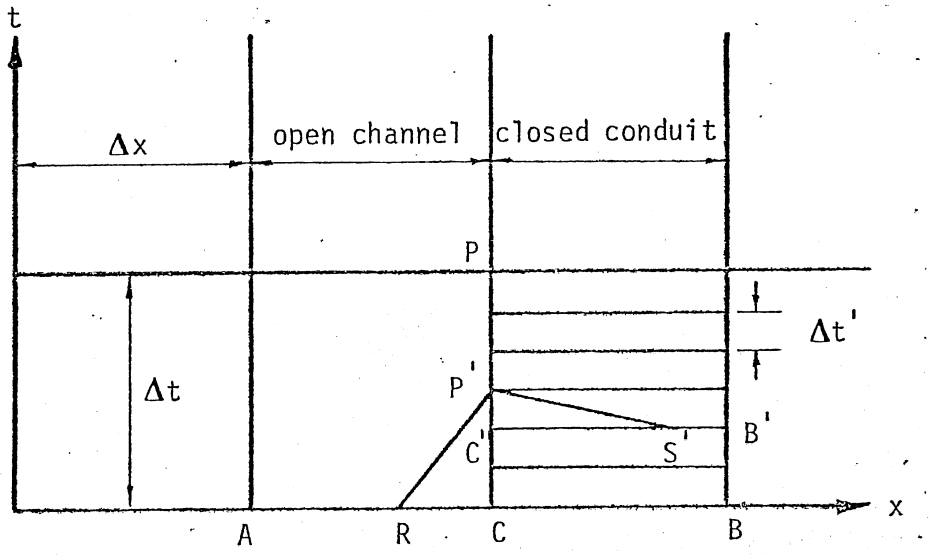

Fig. 3 - Fixed Grid System for Mixed Phase Flow.

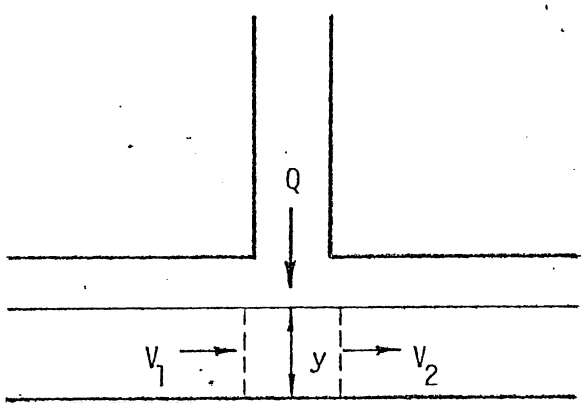

(a) Open channel flow

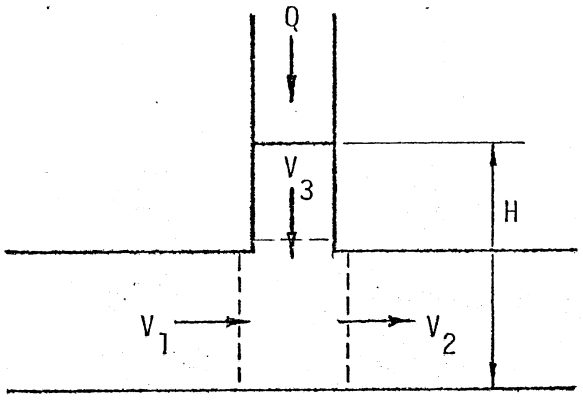

(b) A typical case of closed conduit flow.

Fig. 4 - Flow Conditions at Dropshaft.

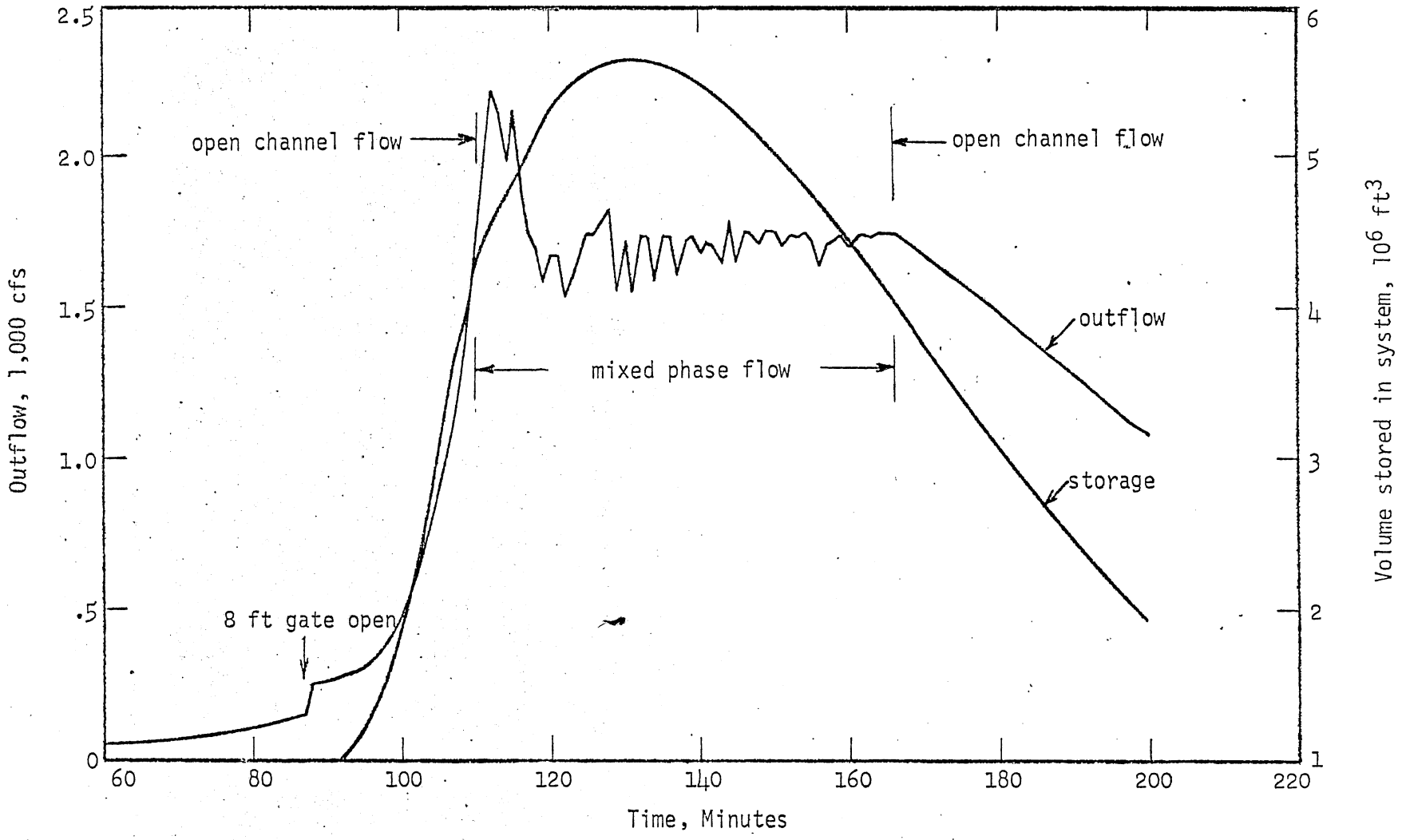

Fig. 5 - Outflow Hydrograph and Storage.

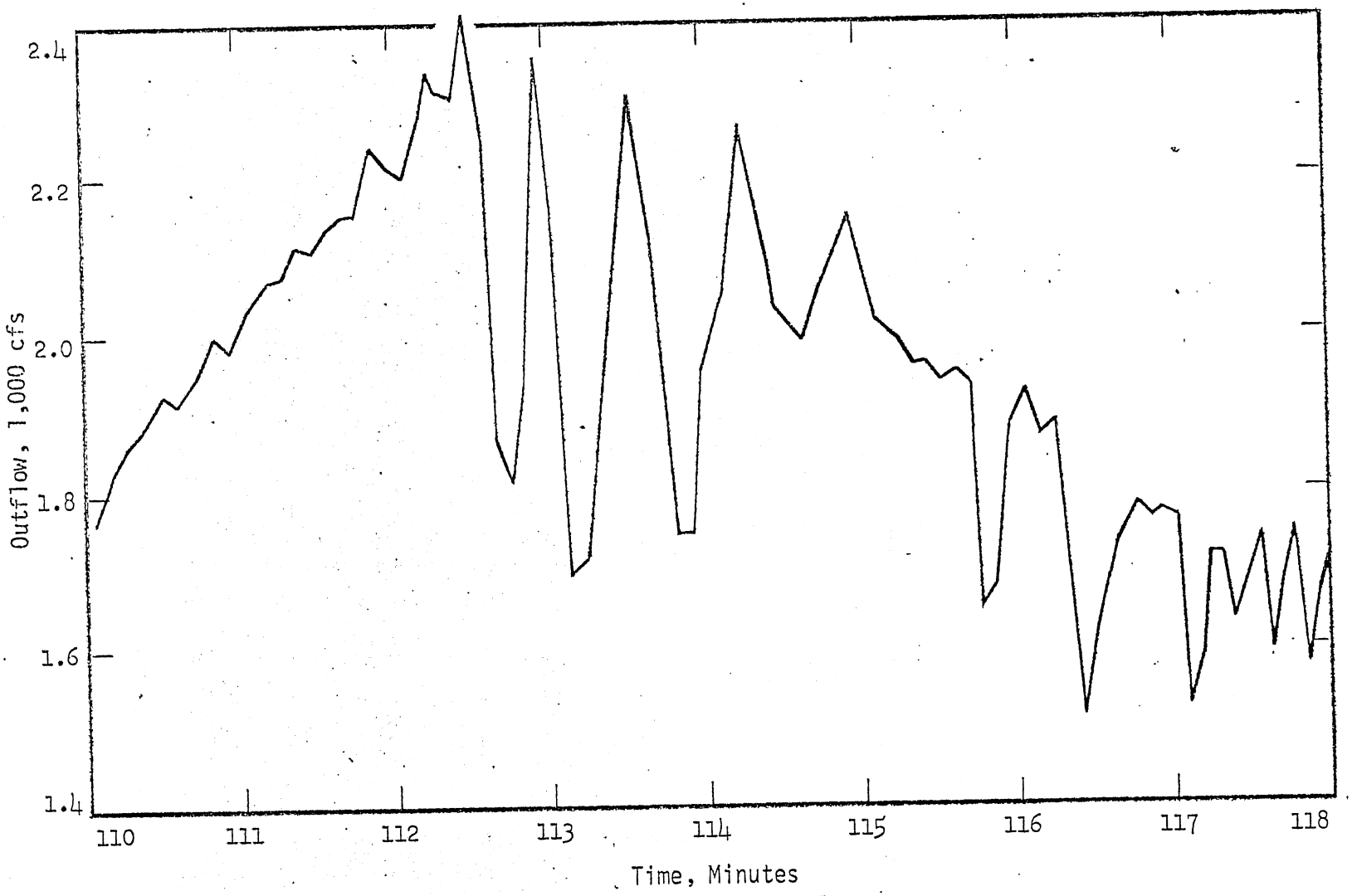

Fig. 6 - Surges near Peak Outflow.

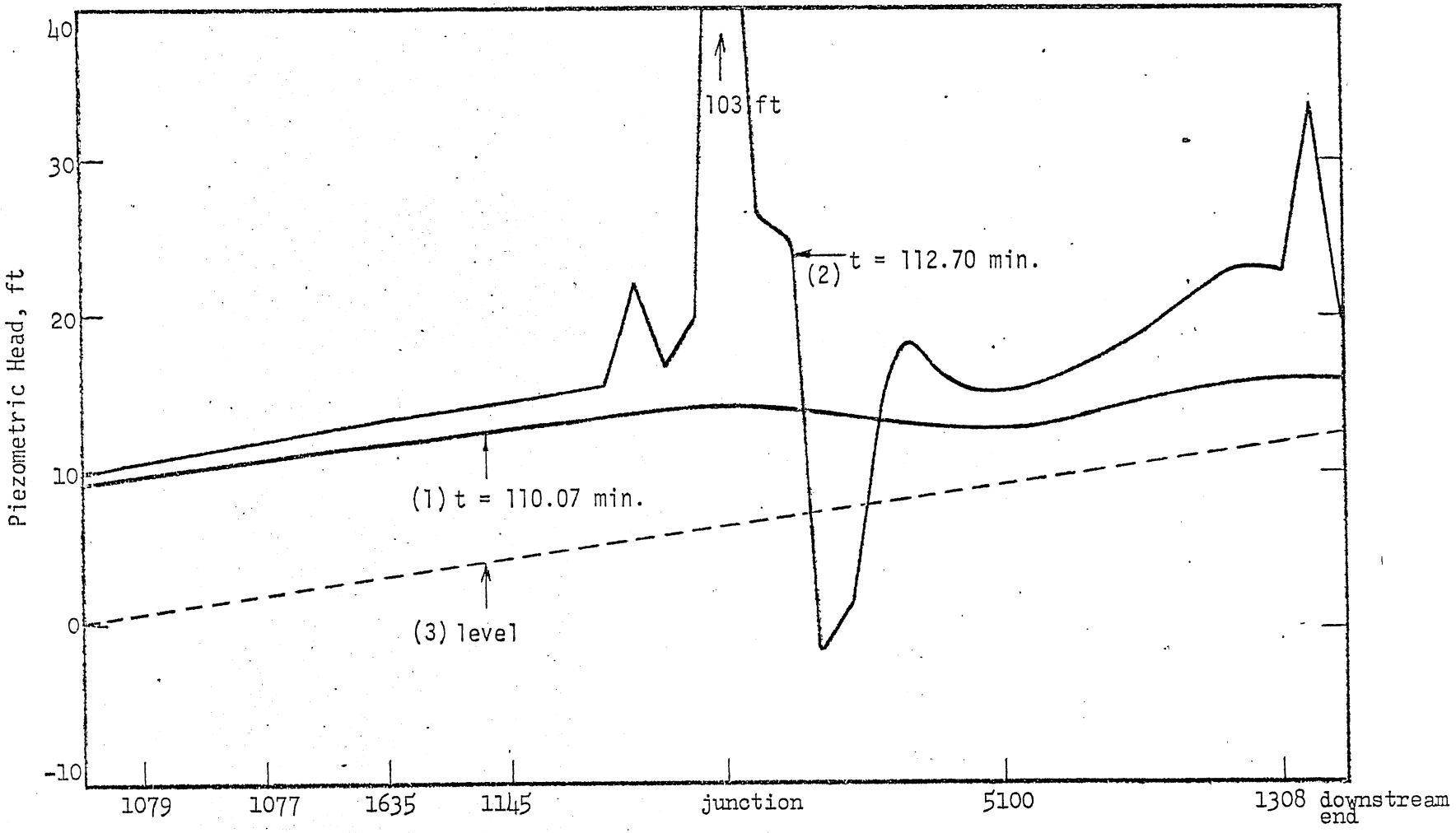

Fig. 7 - Hydraulic Gradelines - Goodman Street.

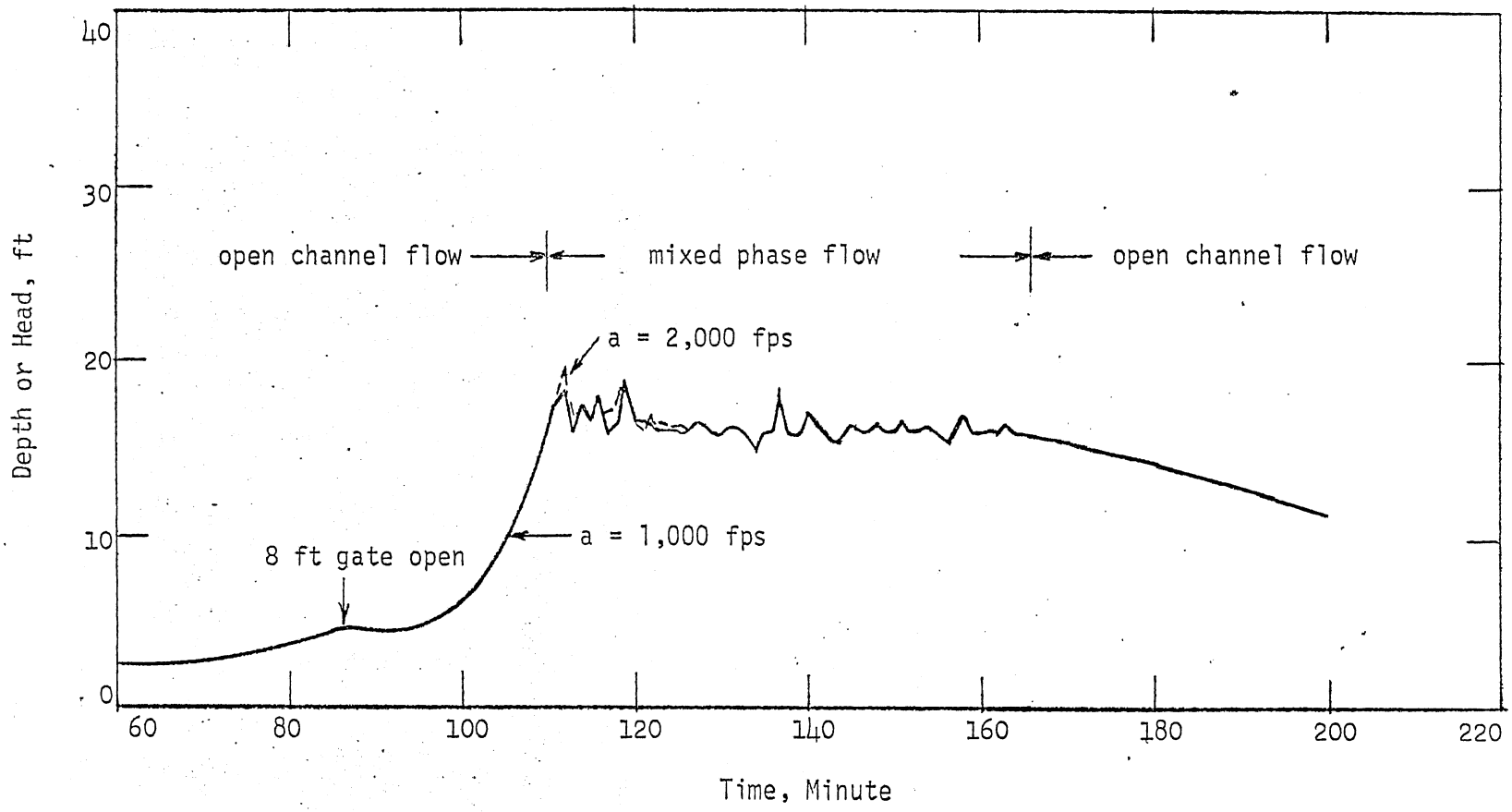

Fig. 8 - Time Record of Flow Depth or Head at the Norton Dropshaft (station 1308).

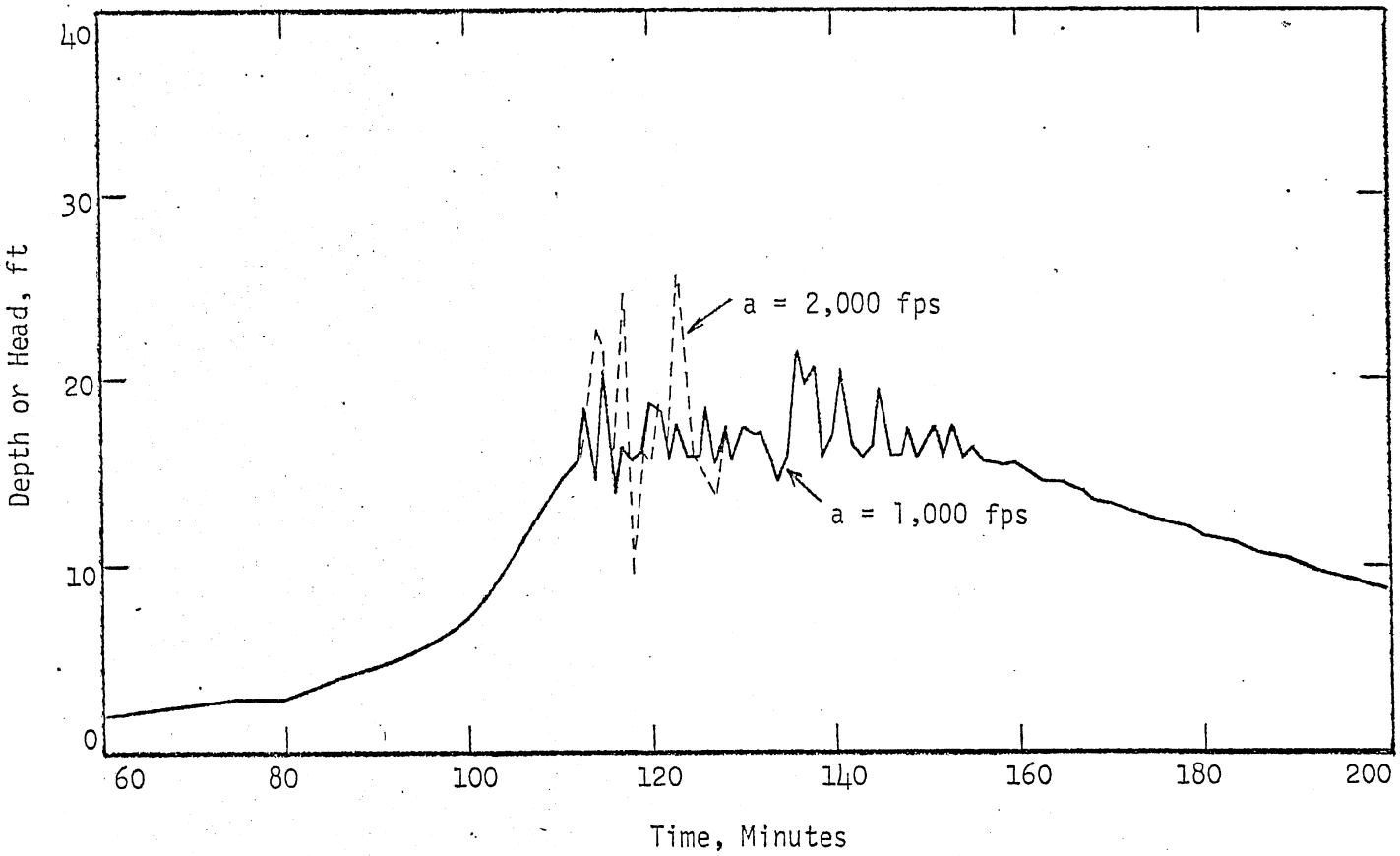

Fig. 9 - Time Record of Flow Depth or Head at the Junction.

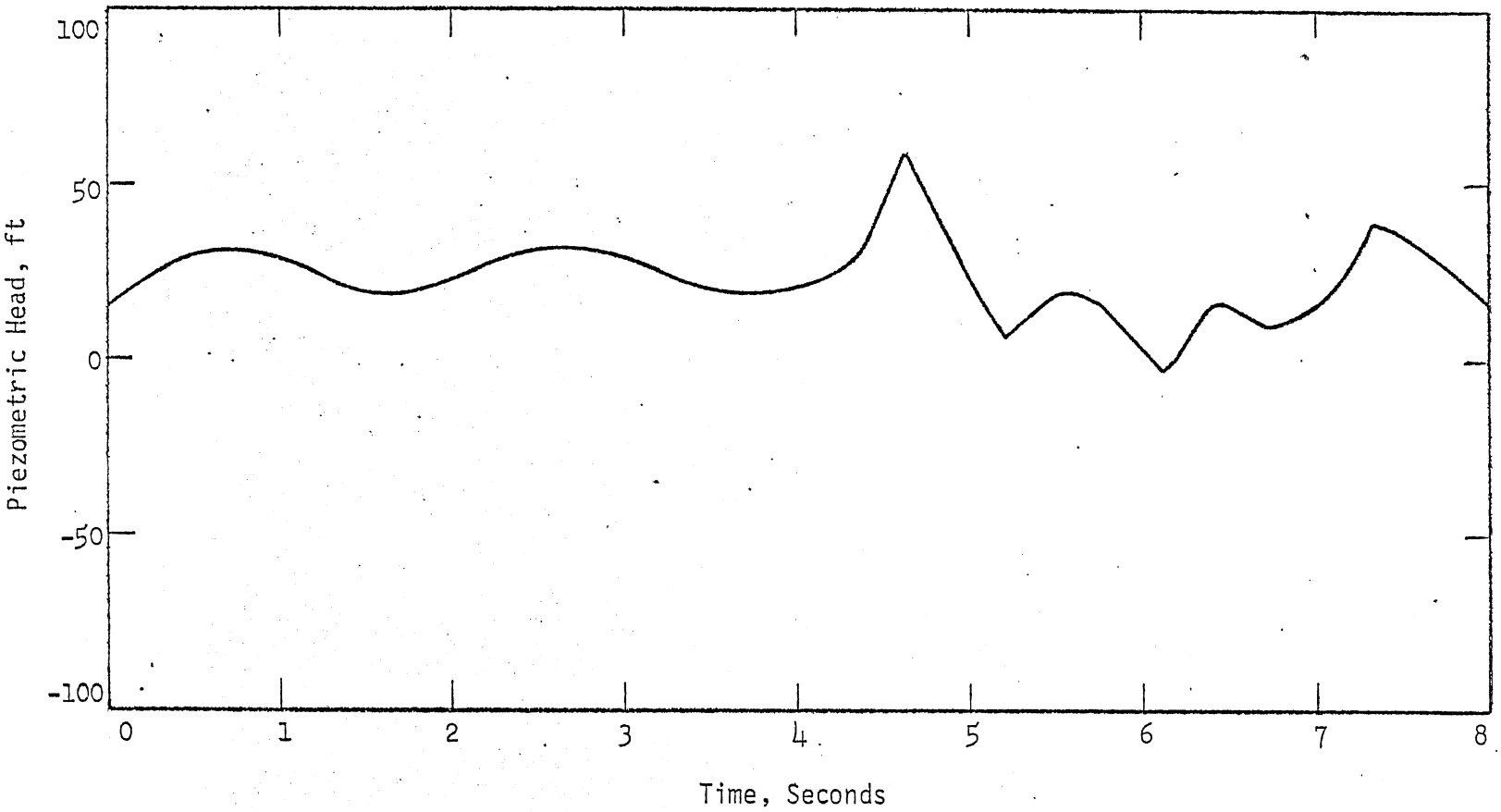

Fig. 10 - Water Hammer Pressure at the Junction, a = 1,000 fps
t = 112.7 + minutes.

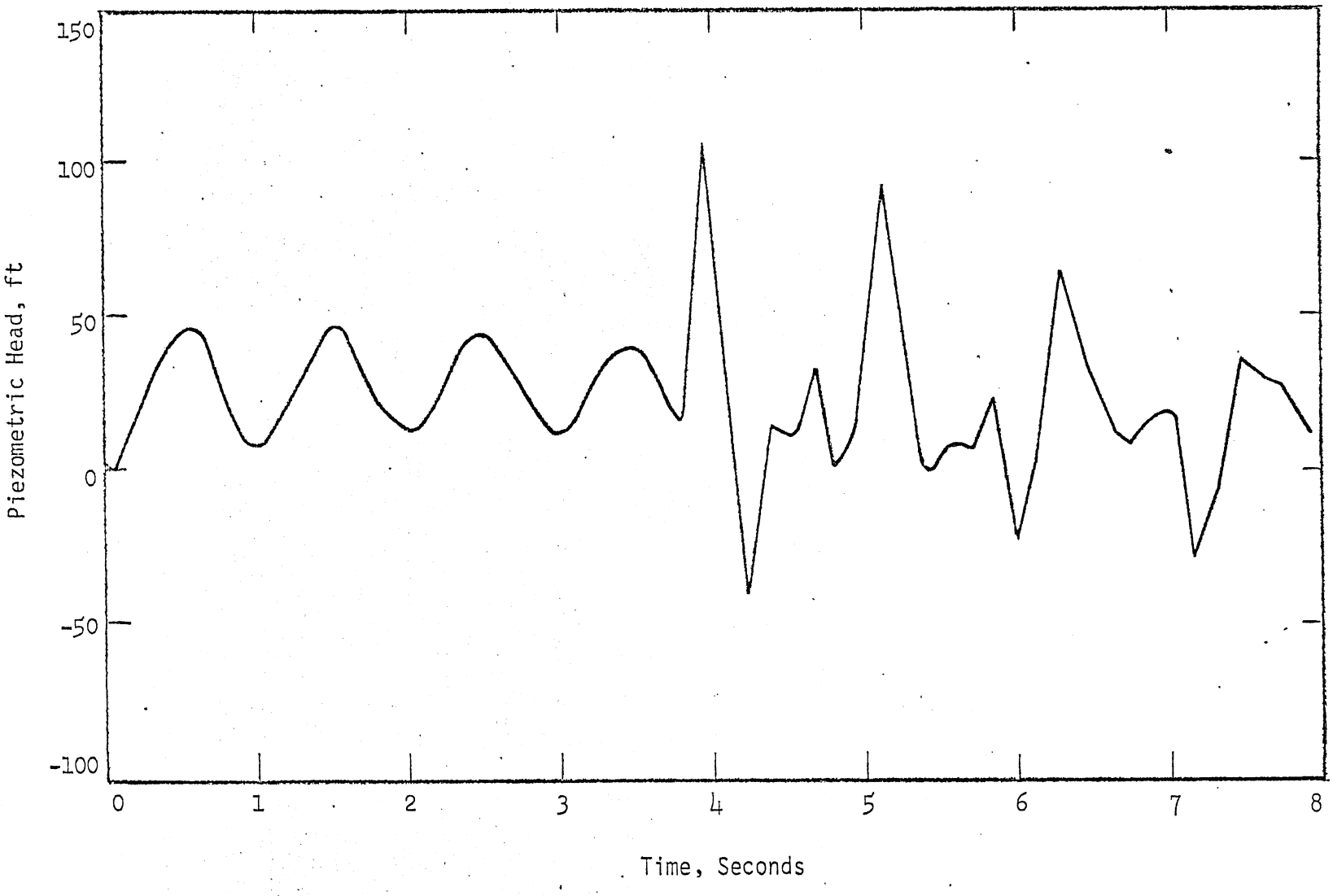

Fig. 11 - Water Hammer Pressure at the Junction, a = 2,000 fps
t = 112.7 + minutes.

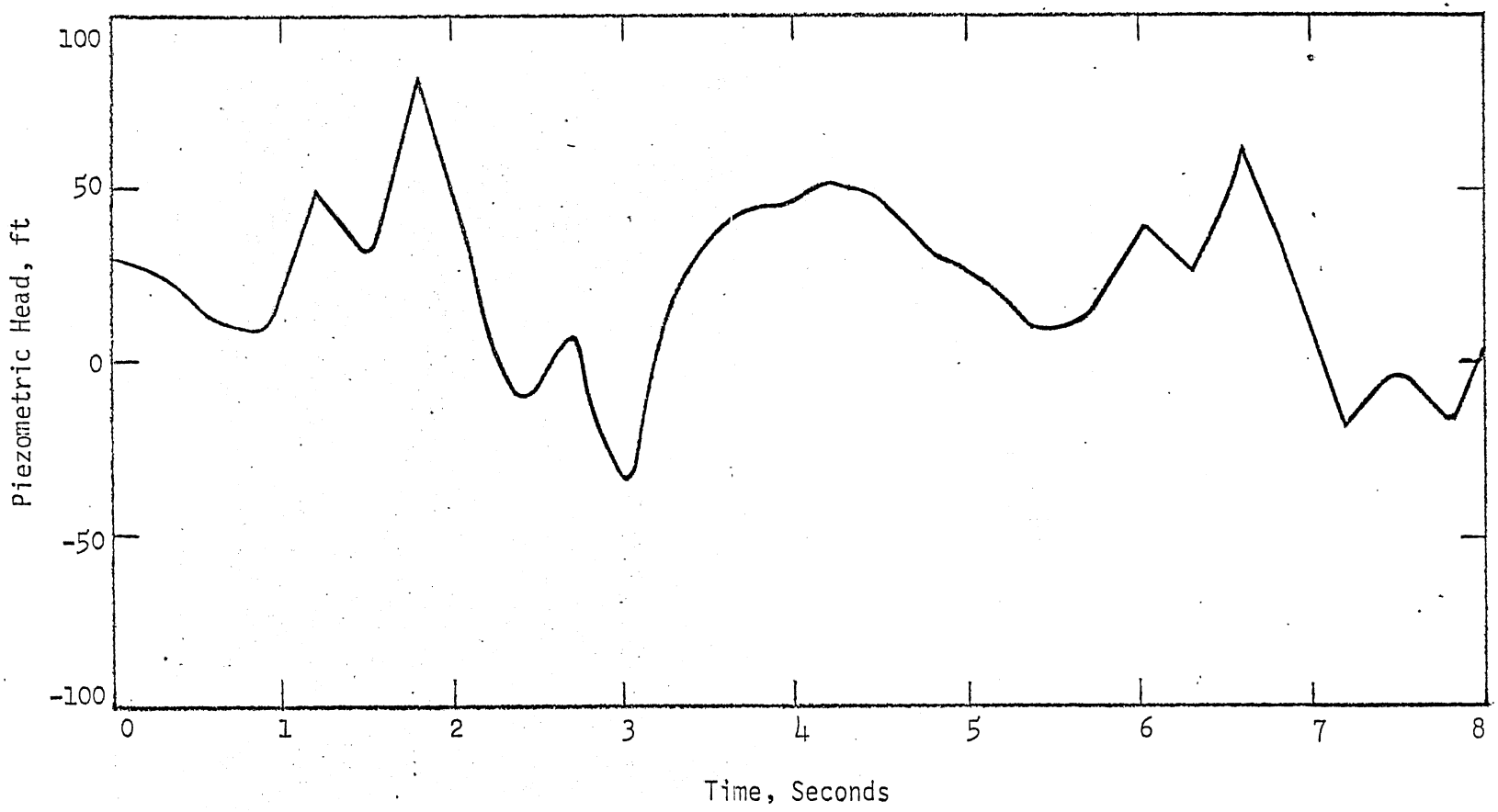

Fig. 12 - Water Hammer Pressure 600 ft Upstream of the Master Street Pump Station (5100), a = 1,000 fps t = 112.3 + minutes.

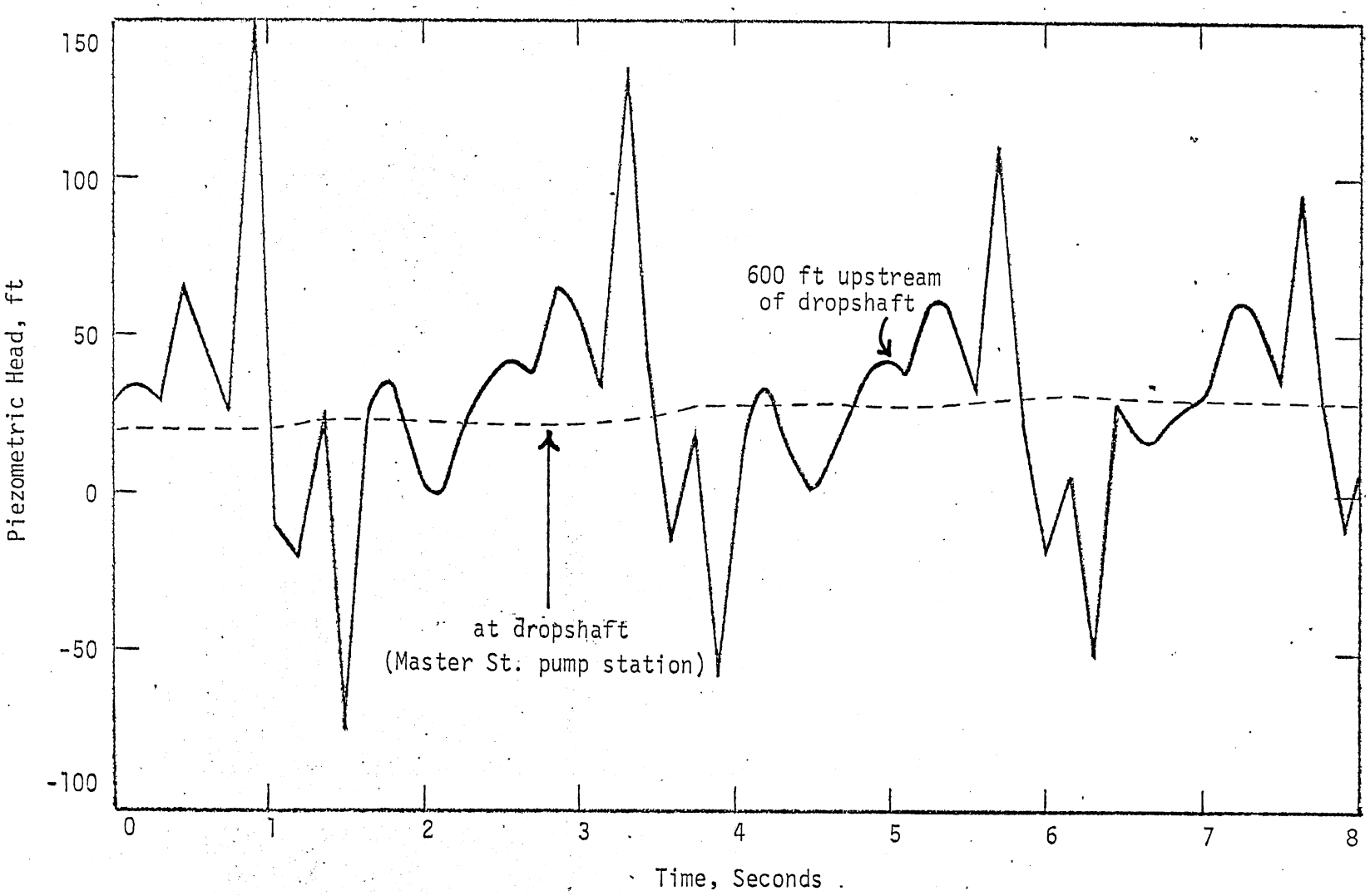

Fig. 13 - Water Hammer Pressure 600 ft Upstream of the Master Street Pump Station, a = 2,000 fps t = 112.3 + minutes.

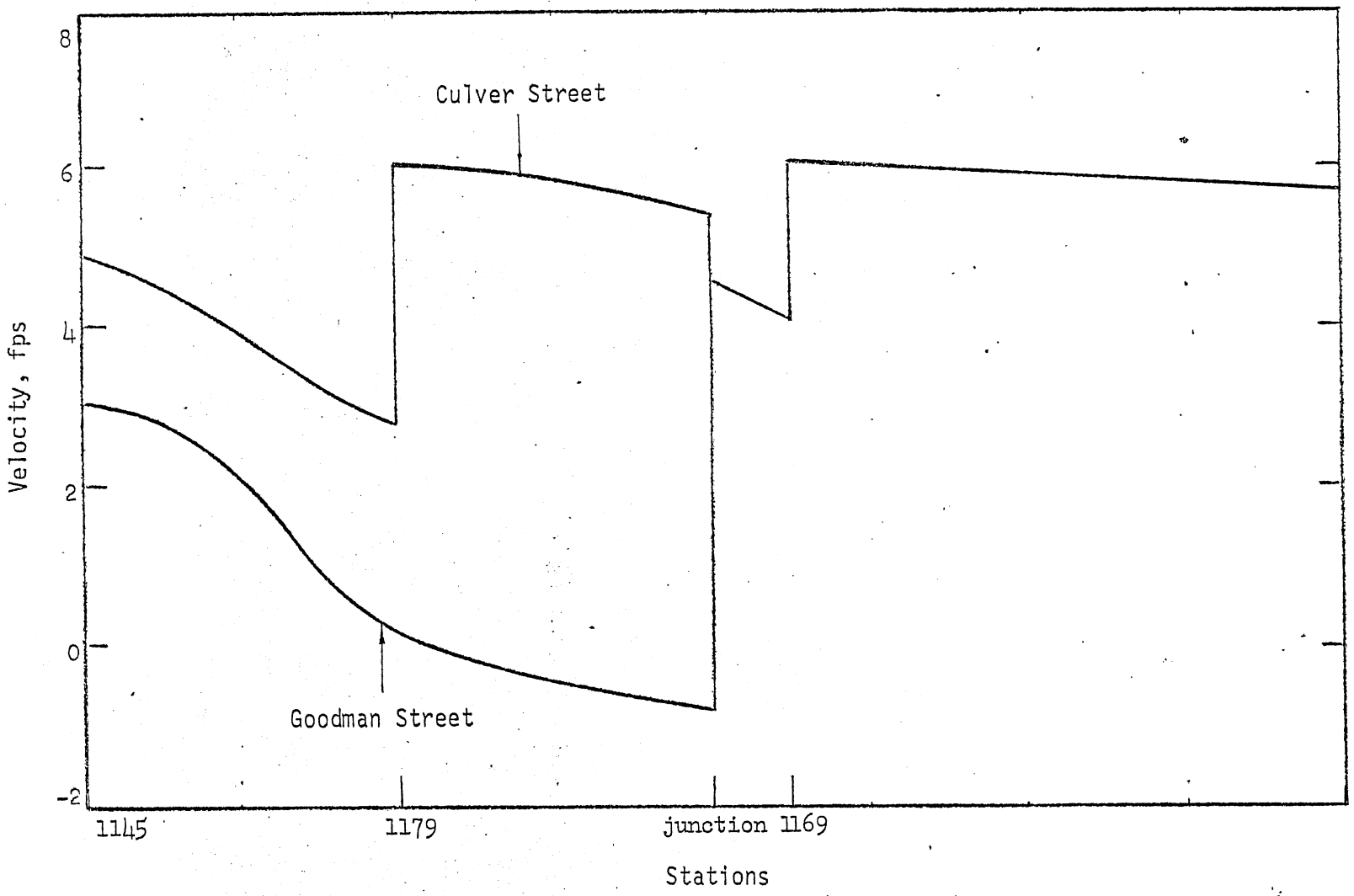

Fig. 14 - Velocity Profile at t = 78.42 minutes.